Central European Journal of Energetic Materials
ISSN 1733-7178; e-ISSN 2353-1843

Cent. Eur. J. Energ. Mater. 2017, *14*(1): 201-216; DOI: 10.22211/cejem/65140

Effect of Nanomaterials on Thermal Stability of 1,3,6,8-Tetranitro Carbazole

Seied Mahdi Pourmortazavi,[1*] Mehdi Rahimi-Nasrabadi,[2] Hossein Rai,[3] Yousef Jabbarzadeh,[1] Abdollah Javidan [3]

[1] *Faculty of Material and Manufacturing Technologies, Malek Ashtar University of Technology, Tehran, Iran*
[2] *Nano Science Center, Imam Hossein University, Tehran, Iran*
[3] *Department of Chemistry, Imam Hossein University, Tehran, Iran*
[*] *E-mail: pourmortazavi@yahoo.com*

Abstract: 1,3,6,8-tetranitro carbazole (TNC) as a secondary explosive is used in composite explosive formulations in order to reduce the sensitivity and increase the stability of the explosive composites. In this work, the thermal stabilities of pure TNC and its nanocomposites prepared via three different nanoparticles were studied by thermal analysis, *i.e.* differential scanning calorimetery (DSC) and thermogravimetry (TG) techniques. Thermal analysis data revealed that the thermal behavior of pure TNC is significantly different from the nanocomposites studied. Pure TNC decomposed completely during a single step in the temperature range 385-425 °C. However, the addition of nanoparticles to the TNC powder leads to higher thermal stability in comparison with the pure TNC. The decomposition kinetics of TNC and its nanocomposites were studied by non-isothermal DSC at several heating rates. Thermokinetic and thermodynamic parameters corresponding to the thermal decomposition of pure TNC and nanocomposites were computed and compared. The results showed that the addition of nanoparticles to the TNC powder has a considerable effect on the thermal stability of the explosive.

Keywords: thermal stability, nanomaterial effect, decomposition kinetics, 1,3,6,8-tetranitro carbazole, energetic material

1 Introduction

1,3,6,8-tetranitro carbazole (TNC), a nitroaromatic explosive with the chemical structure shown in Figure 1, is a secondary nitroaromatic explosive which was

introduced for the first time in earliest decade of the 20th century [1]. During the Second World War TNC was used by Germany as a black powder inhibitor, due to its non-corrosive and hydrophobic properties. Today, TNC commonly is used in explosive composites containing 1,3,5-trinitro-1,3,5-triazine (RDX), and 1,3,5,7-tetranitro-1,3,5,7-tetrazocine (HMX) in order to reduce the sensitivity and increase the stability of these compositions [2, 3]. TNC is also used as an energetic fuel in some propellants and in some pyrotechnic systems as ignitors. Moreover, TNC is employed in car airbags as an initiator and decomposition catalyst [4]. TNC is also known as 'Nitrosane' in civilian industry and used as an insecticide [3, 4].

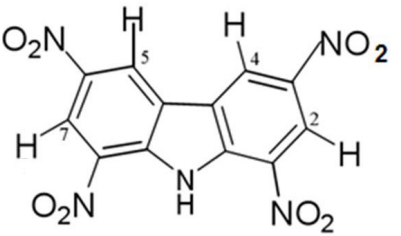

Figure 1. Chemical structure of TNC

Thermal analysis data combined with thermokinetic and thermodynamic results for energetic materials (such as TNC) is essential for safe handling, storage, and use of these hazardous compounds [5-7]. Thermal analysis results can also be analysed using kinetic theory to provide valuable parameters concerning the thermal decomposition of energetic compounds. Examples include suitable mechanisms, decomposition rates, and the values of kinetic and thermodynamic parameters [8, 9]. Furthermore, thermal analysis data permit the prediction of the critical ignition temperature and the shelf-life or half-life for an energetic compound at any given temperature [10-12]. These capabilities make thermal analysis techniques valuable tools in energetic materials characterization.

Organic/inorganic nanocomposites including one or several nanomaterials have been widely investigated in recent years [13-15]. Depending on the number of particles with dimensions in the nanometer range, nanomaterials can be classified into three main categories, *i.e*. nanoparticles, nanotubes and nanolayers [16-18]. Important inorganic nanoscale fillers, which are widely used in nanocomposites, include nanotubes (mainly carbon nanotubes or CNTs), layered silicates (*e.g*. montmorillonite), SiO_2, metal oxides (*e.g.* Al_2O_3, TiO_2, Fe_2O_3), metal nanoparticles (*e.g.* Au, Ag), semiconductors (*e.g.* PbS, CdS), and nanodiamond. All of these nanoparticles have been used in order to enhance

the physical and mechanical properties of composites [19, 20]. The effect of nanoparticles on enhancing the flame retardancy and thermal degradation of nanocomposites is well known [21]. It has been reported that CNTs can encapsulate molecules of target compounds (or provide a strong interaction with them), and the resulting composite can exhibit new properties, *e.g.* a different thermal stability compared to the pure component [19]. On the other hand, Al_2O_3 and TiO_2 (two well- known metal oxides) can have catalytic effects on the thermal decomposition reactions of organic and polymeric compounds, which may lead to a higher or lower stability for the resulting composites [20, 21].

In the first part of this study, the thermal behavior of pure TNC was investigated using thermogravimetery (TG) and differential scanning calorimetery (DSC) techniques. Then, in the second part, the effects of three different nanoscale compounds (Al_2O_3 and TiO_2 nanoparticles and CNTs) on the thermal stability of TNC were studied. In the third part of this work, the thermokinetic and thermodynamic parameters of pure TNC and its composites with nanomaterials were obtained and compared. To the best our knowledge, there is no previous report available on the thermal behavior and degradation kinetics of TNC.

2 Experimental

2.1 Materials and instruments

The wetting solvent n-hexane was purchased from Merck. TNC was synthesized and recrystallized three times from acetone (purity of 99.7%) as reported previously [22]. Multiwall CNTs were obtained from Nanocyl™ NC 7000 (Belgium) and used as received. Aluminum oxide and titanium oxide nanoparticles were prepared in our laboratory by the flame combustion technique as reported previously [23, 24].

Titanium tetraisopropoxide was used as the source of titanium, while hydrated aluminum nitrate was used in the synthesis of alumina nanoparticles. The synthesized TiO_2 and Al_2O_3 nanoparticles were characterized using SEM and XRD. The SEM images obtained are shown in Figure 2. As can be seen in this figure, aluminum oxide and titanium oxide nanoparticles have a (surface) average particle size of 50 nm and 40 nm, respectively.

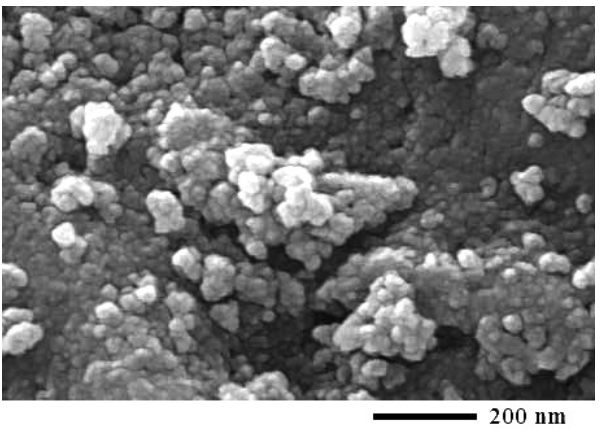

a

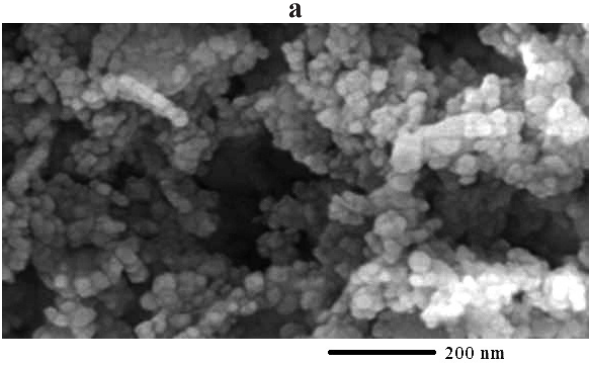

b

Figure 2. SEM images of the synthesized nanoparticles: (a) Al_2O_3, (b) TiO_2

A simultaneous thermal analyzer (STA) instrument including a TG analyzer coupled with a DSC attachment was used for TG/DSC studies. TG/DSC experiments were carried out at a heating rate of 10 $K \cdot min^{-1}$ in nitrogen atmosphere at 1 bar, the sample mass being 4 mg. DSC experiments were performed using a DuPont DSC model 910 at heating rates of 10, 15, 20, and 25 $K \cdot min^{-1}$ from 40 °C up to the end of the decomposition process. DSC measurements were conducted by placing 3 mg samples in an aluminum pan with a perforated lid under a nitrogen atmosphere (flow rate 50 $mL \cdot min^{-1}$).

2.2 Nanocomposites preparation procedure

The preparation of the energetic nanocomposites was carried out via dispersion of each nanomaterial (10% by weight with respect to total amount of TNC) by sonication for 10 min in 10 mL of hexane. Then, the TNC powder was added

to a container containing nanomaterial and hexane. A homogeneous mixture of TNC powder and nanomaterial dispersed in hexane was obtained after about 20 min sonication of the mixture. The hexane was removed from the TNC and nanomaterial mixture using the solvent evaporation method in which the container containing the mixture was connected to a vacuum pump and continuously stirred.

3 Results and Discussion

The prepared nanocomposites were characterized using SEM. The images obtained are presented in Figure S1 (see supporting information). As can be seen in this figure, the nanomaterials are dispersed throughout the matrices of the energetic samples. Afterwards the samples were investigated by thermal analysis techniques to characterize their thermal behavior and thermokinetic parameters.

3.1 Thermal properties of pure TNC and nanocomposites

TG/DSC thermograms for pure TNC samples are shown in Figure 3a. The pure TNC DSC curve shows no change in the thermal pattern of the explosive up to 270 °C. The DSC curve reveals endothermic behavior for TNC near 298 °C. This peak corresponds to the melting point of the energetic compound. At a temperature higher than the melting point (409.7 °C), decomposition of TNC occurred seen as a sharp exothermic peak. This event corresponded to about a 100% loss in the mass of sample as can be seen in the TG thermogram for a pure TNC sample. As can be seen in the DSC curve (Figure 3a) there is a long temperature interval between fusion of TNC at 297.7 °C and its rapid exothermic decomposition at 409.7 °C.

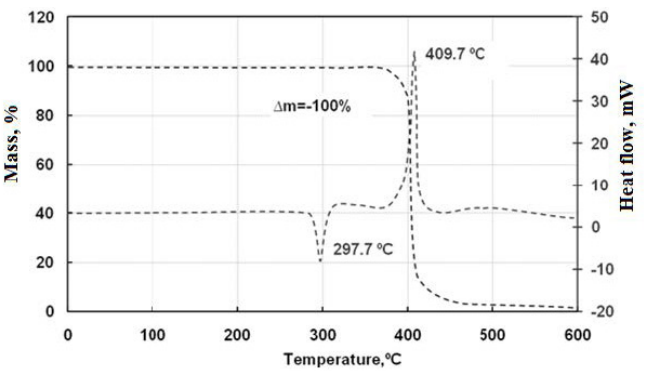

a. TNC

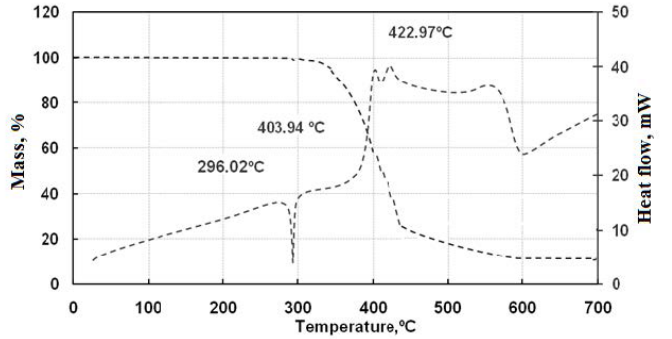

b. TNC/TiO_2

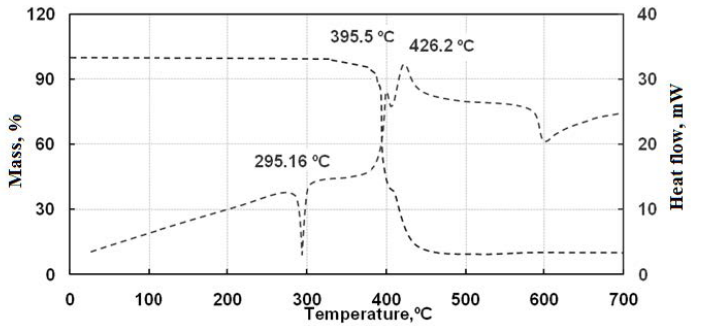

c. TNC/Al_2O_3

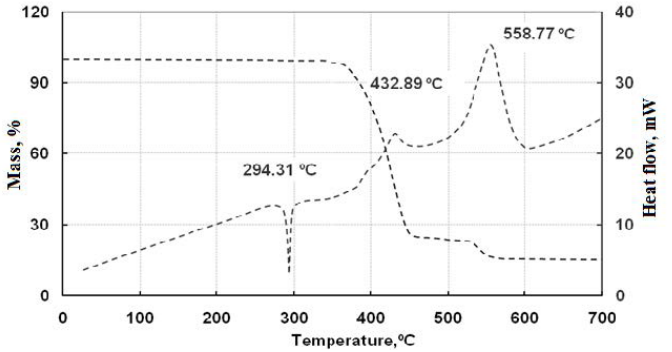

d. TNC/CNT

Figure 3. TG/DSC Curves for TNC Samples: (a) pure TNC (b) TNC/TiO_2 (c) TNC/Al_2O_3 and (d) TNC/CNT; Sample Mass 4.0 mg; Heating Rate 10 $K \cdot min^{-1}$; Nitrogen atmosphere

Simultaneous TG/DSC thermograms for the TNC-TiO_2 nanocomposite are shown in Figure 3b. No thermal event is observed before the melting point of

TNC near 296 °C. However, there are two continuous exothermic peaks above this temperature, corresponding to the decomposition process of TNC. The decomposition process continued until about 550 °C where it reached its end. The completeness of the sample decomposition is confirmed by a TG curve. For this energetic nanocomposite, the first decomposition step occurred at a peak temperature of 403.9 °C. In the second step of the TNC-TiO_2 decomposition process, an exothermic phenomenon was observed at about 423 °C. The TG curve for this sample showed continuous mass loss during these exothermic phenomena with about an 80% decrease in the total mass of the sample.

TG/DSC thermograms for TNC-Al_2O_3 are presented in Figure 3c. The thermal behavior of this nanocomposite is similar to the TNC-TiO_2 sample. In the DSC curve, an endothermic peak and two exothermic peaks were observed at temperatures of 295.2 °C, 395.5 °C and 426.2 °C, respectively. The endothermic peak appearing at 295.2 °C corresponds to the melting of TNC in the mixture and is not associated with any decrease in the sample's mass. By contrast, the first exothermic peak originates at the beginning of the thermal decomposition process of the TNC-Al_2O_3 nanocomposite and the second peak observed at about 426.2 °C is responsible for the final stage of composite decomposition. Here, again the TG curve of the sample showed continuous mass loss during both exothermic phenomena resulting in about 90% decrease in the total mass of the sample.

Figure 3d shows TG and DSC curves for the TNC-CNT nanocomposite. These thermograms confirm that the thermal behavior of this energetic composite is similar to TNC-Al_2O_3 and TNC-TiO_2. This nanocomposite showed endothermic behavior near 294.3 °C (which is the melting point of the TNC in the mixture) without any change in the sample mass occurring in the TG thermogram. Above the melting point, the first step of decomposition occurred at a peak temperature of 432.9 °C. Then, the second step of decomposition for this energetic nanocomposite was observed at a maximum DSC peak temperature of 558.8 °C (which is the decomposition temperature of the CNTs [25]) and caused amplification of the mass loss in this step. These two steps were associated with about 95% sample mass loss in the TG thermogram. A summary of TG/DSC data for the thermal behavior of the energetic nanocomposites is presented in Table 1.

Table 1. Summary of TG/ DSC results for investigated energetic compounds

Compound	Melting [°C]	T^* [°C]	Δm [%]
TNC	297.7	370-420	100
TNC/Al_2O_3	296.4	370-420	80
TNC/TiO_2	296.4	350-460	90
TNC/CNT	295.7	370-530	95

T^* is the temperature range when there is fall in a sample's mass.

3.2 Decomposition kinetics studies using DSC

Thermokinetic and thermodynamic parameters corresponding to the thermal decomposition of pure TNC, TNC-Al_2O_3, TNC-TiO_2 and TNC-CNT samples were obtained by non-isothermal DSC at several heating rates (*i.e.*, 10, 15, 20, and 25 $K \cdot min^{-1}$). DSC thermograms for the decomposition of pure TNC, TNC-Al_2O_3, TNC-TiO_2 and TNC-CNT at different heating rates are shown in Figure S2 (see S.I.). As expected [26], all of the samples investigated showed higher decomposition peak temperatures at higher heating rates. Arrhenius parameters for thermal decomposition of the energetic nanocomposites were determined using the ASTM method E698 [27] via plotting the values of $\ln(\beta \cdot T_m^{-2})$ against $1/T_m$, where β and T_m are respectively the DSC heating rate and maximum DSC peak temperature corresponding to the first step of decomposition reaction. The values of maximum peak temperatures (T_m) for pure TNC, TNC-Al_2O_3, TNC-TiO_2 and TNC-CNT samples at different heating rates (β) are shown in Table S1 (see S.I.). Plotting the values obtained as $\ln(\beta \cdot T_m^{-2})$ *vs.* $1/T_m$ yielded straight lines for pure TNC ($r = 0.991$), TNC-Al_2O_3 ($r = 0.999$), TNC-TiO_2 ($r = 0.999$) and TNC-CNT ($r = 0.999$), which indicates that the thermal decomposition mechanisms of these energetic nanocomposites undergoes no variation during the decomposition process at the heating rates investigated [28, 29]. The activation energy value required for thermal decomposition of each sample was computed from the slopes of these lines ($-E_a/R$). Then, these values of activation energies were used to determine the logarithm of the pre-exponential factor, $\ln(A/s^{-1})$, via the following equation as proposed by ASTM E698:

$$A = \beta \, (E_a/RT_m^2) \, exp(E_a/RT_m) \tag{1}$$

Values of activation energy and frequency factors for pure TNC and energetic nanocomposites were calculated using the ASTM method and the results are presented in Table 2. The activation energies (E_a) for the samples studied were also calculated using the Starink method (another well-known thermokinetic method). In this method, the value of activation energy is obtained by plotting $\ln(\beta \cdot T_m^{-1.92})$ *vs.* $1/T_m$. Fortunately, the Starink method (like the ASTM method) can predict the activation energy of a sample without precise knowledge of the reaction mechanism, via the following expression [30, 31]:

$$\ln(\beta \cdot T_m^{-1.92}) + 1.0008 \, E_a/RT_m = C \tag{2}$$

The plots of $\ln(\beta \cdot T_m^{-1.92})$ versus the reciprocal of the absolute peak temperature for the samples studied produced straight lines with regression

coefficients $r = 0.991$ for pure TNC and $r = 0.999$ for TNC-Al_2O_3, TNC-TiO_2 and TNC-CNT. These results confirm that the thermal decomposition mechanisms of the energetic samples studied do not change much over the heating rates investigated [29]. Thereafter, the values of the frequency factors (A) corresponding to the activation energies obtained by this method for pure TNC and the other energetic nanocomposites were computed using Equation 1. The values of the Arrhenius parameters computed using both the ASTM and Starink methods are presented in Table 2. Comparing the data obtained from these two kinetics methods reveals that the values of activation energy calculated for all the energetic samples studied using the Starink method are slightly higher than those obtained using the ASTM method. However, the trend in activation energy values for the energetic samples shows good agreement between the ASTM Starink methods.

Table 2. Comparison of kinetic parameters for the first step of TNC, TNC-Al_2O_3, TNC-TiO_2 and TNC-CNT thermal decomposition obtained by ASTM and Starink methods

Compound	Method	Activation Energy [KJ·mol^{-1}]	Frequency Factor ln A/s^{-1}	Linear Regression	$\Delta G^{\#}$ [KJ·mol^{-1}]	$\Delta H^{\#}$ [KJ·mol^{-1}]	$\Delta S^{\#}$ [J·mol^{-1}]	ln$K$	T_b [°C]
TNC	ASTM	183.8	13.71	0.991	176.3	177.9	2.2	-18.0	395.1
	Starink	184.0	13.97	0.991	173.1	178.2	7.1	-17.8	395.1
TNC-Al_2O_3	ASTM	84.6	6.0	0.999	176.4	79.0	-145.7	-8.9	373.3
	Starink	85.0	6.0	0.999	176.8	79.4	-145.6	-8.9	373.0
TNC-TiO_2	ASTM	127.1	9.3	0.999	176.6	121.5	-81.4	-13.0	374.9
	Starink	127.5	9.3	0.999	177.0	121.9	-81.4	-13.0	374.7
TNC-CNT	ASTM	373.8	27.6	0.999	178.6	368.0	+268.3	-37.9	373.1
	Starink	374.0	27.6	0.999	178.7	368.1	+268.3	-38.0	373.1

In the next step, the thermodynamic parameters attributed to the activation of the decomposition reactions of pure TNC and the energetic nanocomposites studied were predicted using expressions (3)-(5) while the thermokinetic data computed using the ASTM and Starink methods (shown in Table 2) were used as input data [32-34]:

$$A \exp \frac{-E}{RT} = \nu \exp \frac{-\Delta G^{\neq}}{RT} \tag{3}$$

$$\Delta H^{\neq} = E - RT \tag{4}$$

$$\Delta G^{\neq} = \Delta H^{\neq} - T\Delta S^{\neq} \tag{5}$$

In Equation 3, $\upsilon = K_B T/h$ (where K_B is the Boltzmann constant and h is the Planck constant). Table 2 gives the calculated values of thermodynamic parameters for pure TNC and its energetic nanocomposites. These thermodynamic values are interesting because they were obtained based on the maximum peak temperatures (T_m) of the DSC curves which characterize the highest decomposition rate of TNC and its nanocomposites.

3.3 Determination of reaction rate constants

The rate constant (k) for the decomposition reaction of the samples studied was determined using Equation 6, where the mechanism of the decomposition reactions is assumed to be first order [35, 36]:

$$\ln k = \ln A - E_a/2.3RT \tag{6}$$

The decomposition reaction rate (k) for each of the samples studied was calculated using the values of activation energies (E_a) and frequency factors (A) obtained using the ASTM and Starink methods at a temperature of 25 °C. Table 2 shows the computed values of $\ln k$ for pure TNC and the first decomposition step for the nanocomposites (*i.e.*, TNC-Al_2O_3, TNC-TiO_2 and TNC-CNT samples). Comparison of the TNC reaction rate constant with the TNC-Al_2O_3, TNC-TiO_2 and TNC-CNT reaction rate constants revealed that the rate constant for TNC is considerably higher than that for TNC-CNT. However, this parameter for the TNC-Al_2O_3 and TNC-TiO_2 nanocomposites is higher than for pure TNC. The lower reaction rate constant for TNC-CNT shows that this energetic nanocomposite has a considerably higher half-life rather than pure TNC in an identical condition of storage, while the half-lives of the two other nanocomposites (*i.e.*, TNC-Al_2O_3 and TNC-TiO_2) are lower.

3.4 Critical ignition temperature

The critical ignition temperature (T_b) is an important parameter which is defined as the maximum temperature that a specific compound can be heated to without undergoing thermal runaway [37, 38]. Determining this parameter is essential

to ensure safe storage, handling and process operations for high energetic compounds. This temperature can be estimated from the thermokinetic data (pre-exponential factor, activation energy, and heat of reaction) using combustion theory. In the present study, the critical temperatures for thermal ignition (T_b) of pure TNC, TNC-Al_2O_3, TNC-TiO_2 and TNC-CNT nanocomposites were predicted using Equations 7 and 8 [37]:

$$T_e = T_{e0} + b\phi_i + c\phi_i^2, \quad i = 1 - 4 \tag{7}$$

$$T_b = \frac{E - \sqrt{E^2 - 4ERT_{e0}}}{2R} \tag{8}$$

where b and c in Equation 7 are fitting coefficients, R and E in Equation 8 are the universal gas constant and the activation energy, respectively. Meanwhile, T_{e0} (which is defined as the onset temperature, T_e, corresponding to $\phi_i \rightarrow 0$) was obtained using Equation 7. T_{e0} for pure TNC, TNC-Al_2O_3, TNC-TiO_2 and TNC-CNT was 375.0 °C, 332.3 °C, 347.4 °C, and 363.8 °C, respectively. These calculated temperatures (T_{e0}) were used for the determination of the critical temperatures for thermal explosion (T_b) of pure TNC, TNC-Al_2O_3, TNC-TiO_2 and TNC-CNT via Equation 8. The calculated critical temperatures of the samples studied are shown in Table 2. Comparing the resulting values of critical ignition temperature (T_b) for the nanocomposites and TNC reveals the lower thermal sensitivity of TNC-CNT compared to pure TNC and the comparable sensitivity of TNC-Al_2O_3 and TNC-TiO_2 to pure TNC.

3.5 Comparison of the pure TNC kinetic data with that for nanocomposites

In this work, the thermal stability and decomposition kinetics of pure TNC, TNC-Al_2O_3, TNC-TiO_2 and TNC-CNT nanocomposites were studied under identical conditions. As seen in Figure 3a and Table 1, TNC melts at 297.7 °C and ignites at a higher temperature (409.7 °C) with a complete fall in the mass of the sample. The addition of Al_2O_3 nanoparticles to TNC decreases the melting and decomposition temperatures of TNC to about 295.2 °C and 395.5 °C, respectively. This trend agreed with a previous study [15] which proposed Al_2O_3 could accelerate the decomposition process of organic compounds via a heterogeneous catalysis mechanism. Replacement of Al_2O_3 in the composite by TiO_2 nanoparticles changes the TNC melting temperature to 296.0 °C and the decomposition temperature to around 403.9 °C. This effect occurs because the presence of some oxides (such as TiO_2) may change the decomposition pathway of the organic compounds by

increasing the quantity of releasing heavy components and decreasing the amount of evolved gas [13-15]. Furthermore, these nanoparticles give rise to a high diffusivity and better heat transfer through the bulk sample [15].

However, replacement of TiO_2 in the composite by CNTs causes the melting point to shift to about 294.3 °C and the decomposition temperature to about 432.9 °C. This pattern was observed due to the ability of CNTs to effectively prevent transport of volatile thermal decomposition products out of the nanocomposite by acting as physical barriers [14]. In addition, appropriate interfacial adhesion between the CNTs and the TNC matrix may restrict the thermal motion of the decomposed molecules resulting in further improvement to the thermal stability of the TNC-CNT nanocomposite.

Comparison of the thermal pattern of pure TNC with nanocomposites reveals that the TNC-CNT mixture is more stable than pure TNC. However, two other nanocomposites, *i.e*. TNC-Al_2O_3 and TNC-TiO_2, have a lower thermal stability. Meanwhile, all the nanocomposites studied decomposed via two continuous steps despite pure TNC completely decomposing in a single step. This effect can be confirmed by considering the thermokinetic data shown in Table 2. The thermokinetic data reveals that among the energetic nanocomposites studied only the TNC-CNT has a higher activation energy for its decomposition reaction while the two other nanocomposites have lower activation energies for their decomposition. These results show that Al_2O_3 and TiO_2 nanoparticles have negative effects on the thermal stability of TNC as an energetic material whereas CNT has the reverse effect on the thermal stability of this explosive molecule and enhances its thermal stability.

Comparing the thermodynamic parameters presented in Table 2 shows that the value of $\Delta S^{\#}$ for TNC-CNT is considerably higher than for pure TNC and the other nanocomposites studied. This means that the corresponding activated complex for TNC-CNT decomposition has a lower degree of arrangement (higher entropy) than its initial state, while the TNC-Al_2O_3 material follows an opposite trend. This trend means (according to the theory of activated complex or transition theory [38, 39]) that the thermal decomposition of TNC-CNT can be interpreted as a slow reaction, while that for TNC-Al_2O_3 has a fast reaction rate. On the other hand, the value of $\Delta G^{\#}$ for the decomposition of pure TNC and its energetic nanocomposites are comparable. However, the value of the activation enthalpies ($\Delta H^{\#}$) for the decomposition of pure TNC is considerably lower than that for TNC-CNT but higher than that for TNC-Al_2O_3 and TNC-TiO_2. The values of $\Delta H^{\#}$ and $\Delta G^{\#}$ for all the samples studied are positive which shows that their decomposition reactions are dependent on the introduction of heat and could be carried out as non-spontaneous reactions.

4 Conclusions

The thermal decomposition patterns of pure TNC as a secondary explosive and its composites with various nanomaterials were studied using the DSC and TG techniques. The results showed that the addition of Al_2O_3, TiO_2 and CNT to the TNC explosive has strong effects on its thermal stability. These effects are dependent on the nanomaterial: the various nanomaterials studied had positive and negative effects on the thermal stability of TNC. The values of activation energies for the decomposition of energetic samples obtained via different methods confirm the TG/DSC data and indicate that the thermal stability of the TNC-CNT nanocomposite is higher than pure TNC. However, TNC-Al_2O_3 and TNC-TiO_2 nanocomposites have a lower thermal stability than pure TNC. Also, the TG/DSC thermograms showed that all the nanocomposites studied decompose via two continuous steps, as opposed to pure TNC which decomposes in a single step. Based on the thermal analysis data obtained in the present study, it was found that the energetic nanocomposites and pure TNC have the following relative thermal stability: TNC-CNT > TNC > TNC-TiO_2 > TNC-Al_2O_3.

(S.I.) Supporting Information is available on the WWW under http://www.wydawnictwa.ipo.waw.pl/CEJEM/contents/2017/vol-14-number-1.html

References

[1] Ziersch, P. Ueber einige Carbazolderivate. *Ber. Dt. Chem. Gesellsch*. **1909**, *42*: 3797-3800.
[2] Fedoroff, B. T.; Sheffield, O. E. *Encyclopedia of Explosives and Related Items*. Picatinny, Arsenal **1966**.
[3] Robidoux, P. Y.; Bardai, G.; Paquet, L.; Ampleman, G.; Thiboutot, S.; Hawari, J.; Sunahara, G. I. Phytotoxicity of 2,4,6-trinitrotoluene (TNT) and Octahydro-1,3,5,7-tetranitro-1,3,5,7-Tetrazocine (HMX) in Spiked Artificial and Natural Forest Soils. *Arch. Environ. Contam. Toxicol*. **2003**, *44*: 198-209.
[4] Rahimi-Nasrabadi, M.; Zahedi, M. M.; Pourmortazavi, S. M.; Heydari, R.; Rai, H.; Jazayeri, J.; Javidan, A. Simultaneous Determination of Carbazole-based Explosives in Environmental Waters by Dispersive Liquid-Liquid Microextraction Coupled to HPLC with UV-Vis Detection. *Microchim. Acta* **2012**, *177*: 145-152.
[5] Shamsipur, M.; Pourmortazavi, S. M.; Hajimirsadeghi, S. S. Investigation on Decomposition Kinetics and Thermal Properties of Copper Fueled Pyrotechnic Compositions. *Combust. Sci. Tech.* **2011**, *183*: 575-587.
[6] Santos, A. F. O.; Basílio, J. I. D.; de Souza, F. S.; Medeiros, A. F. D.; Pinto, M. F.;

de Santana, D. P.; Macêdo, R. O. Application of Thermal Analysis in Study of Binary Mixtures with Metformin. *J. Therm. Anal. Calorim*. **2008**, *93*: 361-364.

[7] Pourmortazavi, S. M.; Hosseini, S. G.; Hajimirsadeghi S.S.; Fareghi Alamdari R. Investigation on Thermal Analysis of Binary Zirconium/Oxidant Pyrotechnic Systems. *Combust. Sci. Technol*. **2008**, *180*: 2093-2102.

[8] Asadi, Z.; Nasrollahi, R.; Dusek, M.; Fejfarova, K.; Ranjkeshshorkaei, M.; Dehghani Firuzabadi F. Effect of the Substitutional Groups on the Electrochemistry, Kinetic of Thermal Decomposition and Kinetic of Substitution of Some Uranyl Schiff Base Complexes. *J. Iran Chem. Soc*. **2016**, *13*: 913-924.

[9] Kohsari, I.; Pourmortazavi, S.M.; Hajimirsadeghi, S.S. Non-isothermal Kinetic Study of the Thermal Decomposition of Diaminoglyoxime and Diaminofurazan. *J. Therm. Anal. Calorim.* **2007**, *89*: 543-546.

[10] Shteinberg, A. Thermal Analysis of High-temperature Fast Reactions in Energetic Materials. *J. Therm. Anal. Calorim*. **2011**, *106*: 39-46.

[11] Shamsipur, M.; Pourmortazavi, S.M.; Hajimirsadeghi, S.S.; Atifeh, S.M. Effect of Functional Group on Thermal Stability of Cellulose Derivative Energetic Polymers. *Fuel* **2012**, *95*: 394-399.

[12] Xu, Z.; Zhu, J.; Liao, X.; Ni, H. Thermal Behavior of Poly(ethylene terephthalate)/SiO_2/TiO_2 Nano Composites Prepared via in situ Polymerization. *J. Iran Chem. Soc*. **2015**, *12*: 765-770.

[13] Laachachi, A.; Leroy, E.; Cochez, M.; Ferriol, M.; Lopez Cuesta, J.M. Use of Oxide Nanoparticles and Organoclays to Improve Thermal Stability and Fire Retardancy of Poly(methyl methacrylate). *Polym. Degrad. Stab*. **2005**, *89*: 344-352.

[14] Bikiaris, D. Can Nanoparticles Really Enhance Thermal Stability of Polymers? Part II: An Overview on Thermal Decomposition of Polycondensation Polymers. *Thermochim. Acta* **2011**, *523*: 25-45.

[15] Laachachi, A.; Cochez, M.; Leroy, E.; Gaudon, P.; Ferriol, M.; Lopez Cuesta, J. M. Effect of Al_2O_3 and TiO_2 Nanoparticles and APP on Thermal Stability and Flame Retardance of PMMA. *Polym. Adv. Technol*. **2006**, *17*: 327-334.

[16] Pourmortazavi, S. M.; Hajimirsadeghi, S. S.; Kohsari, I.; Fareghi Alamdari, R.; Rahimi-Nasrabadi, M. Determination of the Optimal Conditions for Synthesis of Silver Oxalate Nanorods. *Chem. Eng. Technol*. **2008**, *31*: 1532-1535.

[17] Alexandre, M.; Dubois, P. Polymer-layered Silicate Nanocomposites: Preparation, Properties and Uses of a New Class of Materials. *Mater. Sci. Eng. R: Rep*. **2000**, *28*: 1-63.

[18] Pourmortazavi, S.M.; Hajimirsadeghi, S.S.; Rahimi-Nasrabadi, M. Statistical Optimization of Condition for Synthesis Lead Sulfide Nanoparticles. *Mater. Manuf. Process*. **2009**, *24*: 524-528.

[19] Paul, D.R.; Robeson, L.M. Polymer Nanotechnology: Nanocomposites. *Polymer* **2008**, *49*: 3187-3204.

[20] Kumar, A. P.; Depan, D.; Tomer, N. S.; Singh R. P. Nanoscale Particles for Polymer Degradation and Stabilization-Trends and Future Perspectives. *Prog. Polym. Sci*. **2009**, *34*: 479-515.

[21] Le Bras, M.; Wilkie, C.; Bourbigot, S.; Duquesne, S. *Fire Retardance of Polymers: The Use of Micro- and Nano-sized Mineral Fillers.* Royal Society of Chemistry, Cambridge **2004**; ISBN: 978-0-85404-149-7.
[22] Pafaff, K.; Erienbach, M.; Finenbrink, W. *Insecticides*. Patent US 2 375 382, **1945**.
[23] Sathyaseelan, B.; Baskaran, I.; Sivakumar, K. Phase Transition Behavior of Nanocrystalline Al_2O_3 Powders. *Soft Nanoscience Letters* **2013**, *3*: 69-74.
[24] Mahender, C.; Murali, B.; Himabindu, V. Synthesis of Nano Phase Titanium Dioxide (TiO_2) in Diffusion Flame Reactor and it Application in Photocatalytic Reaction. *Int. J. Eng. Res*. *Appl.* **2014**, *4*: 209-213.
[25] Hsieh, Y.-C.; Chou, Y.-C.; Lin, C.-P.; Hsieh, T.-F.; Shu, C.-M. Thermal Analysis of Multi-walled Carbon Nanotubes by Kissinger's Corrected Kinetic Equation. *Aerosol Air Qual. Res*. **2010**, *10*: 212-218.
[26] Pourmortazavi, S. M.; Kohsari, I.; Teimouri, M. B.; Hajimirsadeghi, S. S. Thermal Behaviour Kinetic Study of Dihydroglyoxime and Dichloroglyoxime. *Mater. Lett*. **2007**, *61*: 4670-4673.
[27] Kissinger, H. E. Reaction Kinetics in Differential Thermal Analysis. *Anal. Chem*. **1957**, *29*: 1702-1709.
[28] Shamsipur, M.; Pourmortazavi, S. M.; Fathollahi, M. Kinetic Parameters of Binary Iron/Oxidant Pyrolants. *J. Energ. Mater*. **2012**, *30*: 97-106.
[29] Vyazovkin, S.; Burnham, A. K.; Criado, J. M.; Pérez-Maqueda, L. A.; Popescu, C.; Sbirrazzuoli, N. ICTAC Kinetics Committee Recommendations for Performing Kinetic Computations on Thermal Analysis Data. *Thermochim. Acta* **2011**, *520*: 1-19.
[30] Starink, M. J. The Determination of Activation Energy from Linear Heating Rate Experiments: A comparison of the Accuracy of Isoconversion Methods. *Thermochim. Acta* **2003**, *404*: 163-176.
[31] Criado, J. M.; Perez-Maqueda, L. A.; Sanchez-Jimenez, P. E. Dependence of the Preexponential Factor on Temperature. *J. Therm. Anal. Calorim*. **2005**, *82*: 671-675.
[32] Pourmortazavi, S. M.; Rahimi-Nasrabadi, M.; Kohsari, I.; Hajimirsadeghi, S.S. Non-isothermal Kinetic Studies on Thermal Decomposition of Energetic Materials. *J. Therm. Anal. Calorim*. **2012**, *110*: 857-863.
[33] Rodgers, R. N.; Janney, J. L.; Ebinger, M. H. Kinetic-isotope Effects in Thermal Explosions. *Thermochim. Acta* **1982**, *59*: 287-291.
[34] Humienik, M.O.; Mozejko, J. Thermodynamic Functions of Activated Complexes Created in Thermal Decomposition Processes of Sulphates. *Thermochim. Acta* **2000**, *344*: 73-79.
[35] Shamsipur, M.; Pourmortazavi, S.M.; Roushani, M.; Miran Beigi, A.A. Thermal Behavior and Non-isothermal Kinetic Studies on Titanium Hydride-fueled Binary Pyrotechnic Compositions. *Combust. Sci. Technol*. **2013**, *185*: 122-133.
[36] Krabbendam-LaHaye, E.L.M.; de Klerk, W.P.C.; Krämer, R.E. The Kinetic Behaviour and Thermal Stability of Commercially Available Explosives. *J. Therm. Anal. Calorim*. **2005**, *80*: 495-501.

[37] Gao, H.-X.; Zhao, F.-Q.; Hu, R.-Z.; Zhao, H.-A.; Zhang, H. Estimation of the Critical Temperature of Thermal Explosion for Azido-acetic-acid-2-(2-azido-acetoxy)-ethylester Using Non-isothermal DSC. *J. Therm. Anal. Calorim*. **2009**, *95*: 477-483.
[38] Sućeska, M. A Computer Program Based on Finite Difference Method for Studying Thermal Initiation of Explosives. *J. Therm. Anal. Calorim*. **2002**, *68*: 865-875.
[39] Shamsipur, M.; Pourmortazavi, S.M.; Miran Beigi, A.A.; Heydari, R.; Khatibi, M. Thermal Stability and Decomposition Kinetic Studies of Acyclovir and Zidovudine Drug Compounds. *AAPS Pharm. Sci. Tech*. **2013**, *14*: 287-293.